



ORIGINAL ARTICLE

A new methodology to assess the structural capacity of bridge portfolios: application in Northeastern Brazilian bridges

Uma nova metodologia para avaliação da capacidade estrutural de portfólios de pontes: aplicação nas pontes situadas no Nordeste do Brasil

Gustavo Henrique Ferreira Cavalcante^a

Eduardo Marques Vieira Pereira^a

Isabela Durci Rodrigues^b

Luiz Carlos Marcos Vieira Júnior^a

Gustavo Henrique Siqueira^a

^aUniversidade Estadual de Campinas – Unicamp, Faculdade de Engenharia Civil, Arquitetura e Urbanismo, Departamento de Estruturas, Campinas, SP, Brasil

^bUniversidade de São Paulo – USP, Escola de Engenharia de São Carlos, Departamento de Estruturas, São Carlos, SP, Brasil

Received 12 November 2021

Accepted 03 March 2022

Abstract: This article presents a new proposal to estimate structural capacity models for bridge portfolios. A common approach is the use of ductility-based capacity models. Herein, a ductility replacement for curvature or drift as engineering demand parameters is conducted, as variability within the bridge's classes is considered in the results and multidirectional pushover analyses are performed to assess a bi-directional load scenario. Application of the methodology is exemplified for an inventory of Northeastern Brazilian bridges. Parametric analyses are performed by varying the reinforcement ratios to estimate the capacity limit states within the range of values used. These results from probabilistic models define the capacity limit state that can be used to perform vulnerability assessment of bridges to different hazard sources, such as earthquakes.

Keywords: structural capacity, parametric analysis, multidirectional pushover analysis.

Resumo: Este artigo apresenta uma proposta para determinação da capacidade estrutural de portfólios de pontes. Uma prática comum é o uso de modelos de capacidade baseados na ductilidade. Neste trabalho, a ductilidade é substituída por curvatura ou *drift* como parâmetros de demanda, uma vez que a variabilidade dos parâmetros que definem classes de pontes é considerada nos resultados e análises multidirecionais do tipo *Pushover* são realizadas para avaliar cenários de forças bidirecionais. Uma aplicação da metodologia é exemplificada para um inventário de pontes típicas situadas no Nordeste do Brasil. Análises paramétricas são realizadas por meio da variação das taxas de armaduras para determinação dos estados-limites dentro dos valores estudados. Os resultados dos estados limites de capacidade são informações valiosas para realização de estudos de vulnerabilidade de portfólios de pontes para diferentes fontes de ameaça, como sismos.

Palavras-chave: capacidade estrutural, análise paramétrica, pushover multidirecional.

How to cite: G. H. F. Cavalcante, E. M. V. Pereira, I. D. Rodrigues, L. C. M. Vieira Júnior, and G. H. Siqueira, "A new methodology to assess the structural capacity of bridge portfolios: application in Northeastern Brazilian bridges," *Rev. IBRACON Estrut. Mater.*, vol. 16, no. 1, e16101, 2023, <https://doi.org/10.1590/S1983-41952023000100001>

Corresponding author: Gustavo Henrique Ferreira Cavalcante. E-mail: ghenriquefc@hotmail.com

Financial support: This study was financed in part by the Coordenação de Aperfeiçoamento de Pessoal de Nível Superior - Brasil (CAPES) - Finance Code 001; and by the São Paulo Research Foundation (FAPESP) - Finance Code 2018/23304-9. The opinions, findings, and conclusions or recommendations expressed in this paper are those of the authors only and do not necessarily reflect the views of the sponsors or affiliates.

Conflict of interest: Nothing to declare.

Data Availability: The data that support the findings of this study are available from the corresponding author, GHFC, upon reasonable request.



This is an Open Access article distributed under the terms of the Creative Commons Attribution License, which permits unrestricted use, distribution, and reproduction in any medium, provided the original work is properly cited.

1 INTRODUCTION

Bridges have fundamental importance in the economic and social development of cities. Such structures, based on past earthquake events, can be considered the most vulnerable components in a highway transportation system, as highlighted by well-known cases of earthquakes [1]-[3], and other natural hazards [4]-[8]. In order to assess the seismic vulnerability of bridges, Performance-based earthquake engineering (PBEE) can be used, since it is a comprehensive framework of vulnerability in terms of the expected performance [9].

As an essential part of the PBEE framework, there are the fragility functions, which are defined as the conditional probability of damage over a range of potential hazard intensities. Therefore, these functions are important tools in several analyses, such as in regional seismic risk assessments to estimate the potential for damage or losses due to seismic events, or in evaluating the efficiency of seismic design provisions. Fragility assessment requires the probabilistic distributions of the demand and the capacity of each component of the system. The demand is the peak structural response for a given intensity measure, whereas the capacity depicts the response at the limit states' thresholds. Therefore, in order to generate reliable fragility functions, one needs reliable capacity models for all bridge components (e.g., bearing, abutments, columns, deck). Traditionally, these models have been defined in terms of qualitative damage states such as slight, moderate, extensive and complete [10] associated with a timeline for the restoration of the bridge functionality [11].

The columns of a bridge are commonly adopted as a system's component, since severe damage to them may lead to bridge closure or collapse [12]; hence, an adequate determination of the bents' structural capacity probabilistic model is of utmost importance. Most studies on fragility analysis of bridges measure damage based on the column's ductility demand ratio [13], i.e., the ratio of the peak structural response and the structural response that causes the first yield on a reinforcement bar (yield parameter hereafter). Several researchers [9], [11]-[16] adopt the curvature ductility (μ_ϕ) as an engineering demand parameter (EDP) to define column capacity models. This methodology provides probabilistic distributions to properly account for uncertainties about the association between quantitative (e.g., curvature ductility values) and qualitative damage states. For that, it is necessary to associate expert opinion regarding post-event failures [17] and numerical or experimental results [13], [18], [19].

A fragility assessment based on the column's ductility demand ratio requires an adequate definition of the yield parameter (e.g., yield curvature, yield drift, yield displacement). Therefore, analytical equations based on experimental results [20]-[23] or numerical approaches through sectional analysis [24] and Pushover analysis (PA) [25] are commonly adopted. PA is also used to define the limit state models of several types of structural systems, such as buildings [26], bridges [27], and free-form shells [28].

PA consists of the application of incremental forces to evaluate the inelastic behavior of a structure in each step until collapse, or whether any desired displacement, is reached. This procedure allows the definition of the exact step corresponding to the first yield of reinforcing steel, which provides the yield parameter considering the three-dimensional behavior of the structural system and the section properties in the numerical modeling.

Bridges' bents situated in one plane only (e.g., two-column bents) combined with a flexible superstructure using elastomeric bearings can be sensitive to torsion [27]. In addition, ground motions comprise three translational components, which means that simultaneous seismic demand imposes itself in more than one direction (consequently a large resultant demand). Bi-directional loading also increases the strength and stiffness degradation of columns [29]-[30]; therefore, the structural capacity model should be consistently able to reflect this behavior. This means that the traditional methods [20]-[24] may not be adequate to estimate the capacity of bridge bents; however, a multidirectional Pushover procedure can adequately estimate the yield parameter for bi-directional horizontal loads.

In view of the above, this article aims to propose a new probabilistic framework to determine the structural capacity model of bridge's bents coupled with Multidirectional Pushover Analyses (MPA). Nonlinear numerical simulations are conducted using finite element models with features of bridges in Northeastern Brazil, obtained from a robust background statistical study. The MPA are performed to investigate the effect of bi-directional loads on the yield parameter of bridge's bents in Northeastern Brazil. Given that information on the detailing of the existing bridges' bents is hardly available, parametric analyses are also performed to investigate the impact of the column's reinforcement ratios on the yield parameter. The contribution of this study is, therefore, multifold, in the sense that it provides not only insights on the effect of MPA and other parameters in the structural capacity probabilistic models, but also contributes to the development of capacity models for bridges through a new methodology.

2 BRIDGE CHARACTERISTICS AND NUMERICAL MODELING

2.1 Characteristics and variability of bridges

There are approximately 5000 bridges located on federal highways in Brazil, under the supervision of the National Department of Infrastructure and Transportation (DNIT). About 50% of these bridges are located in Northeastern Brazil, which presents one of the highest seismic activities compared to other parts of Brazil [31]-[33]. Furthermore, bridges have the worst structural condition countrywide; 6.6% of them require immediate or mid-term interventions, as seen in [34]. Recurrent floods in the region also aggravate bridges' condition [7]. These specific effects, however, are not explored herein.

A recent study conducted by [35] evaluated 250 reports of bridges located in Northeastern Brazil and grouped them into classes with similar structural characteristics. Table 1 presents the description and representativeness of the bridges' classes, according to the number and spans' continuity, deck section, number of columns per bents, and type of abutments. Cast-in-place and straight concrete bridges supported on elastomeric bearings represent these classes, since they represent the vast majority of the reports.

Table 1. Representativeness and description of the bridges' classes.

Bridge's class	Bridge description	%
SS-SD-Abut	Single-span, slab deck and non-integral abutments	16.4%
SS-TB-Abut	Single-span, T-beam deck and non-integral abutments	27.6%
MSC-TB	Multi-span continuous, T-beam deck, two column bents and no abutments	17.2%
MSC-TB-Abut	Multi-span continuous, T-beam deck, two column bents and non-integral abutments	6.4%
Others		32.4%

Two bridges' classes with bents (MSC-TB and MSC-TB-Abut) are analyzed herein and represent 23.6% of the total of the selected bridges (250). Figure 1 illustrates the geometric properties of the typical bridges' classes described in Table 1. Gravity or U seat-type abutments support MSC-TB-Abut bridge's classes. All decks of the bridges' classes (MSC-TB and MSC-TB-Abut) are considered supported on elastomeric bearings.

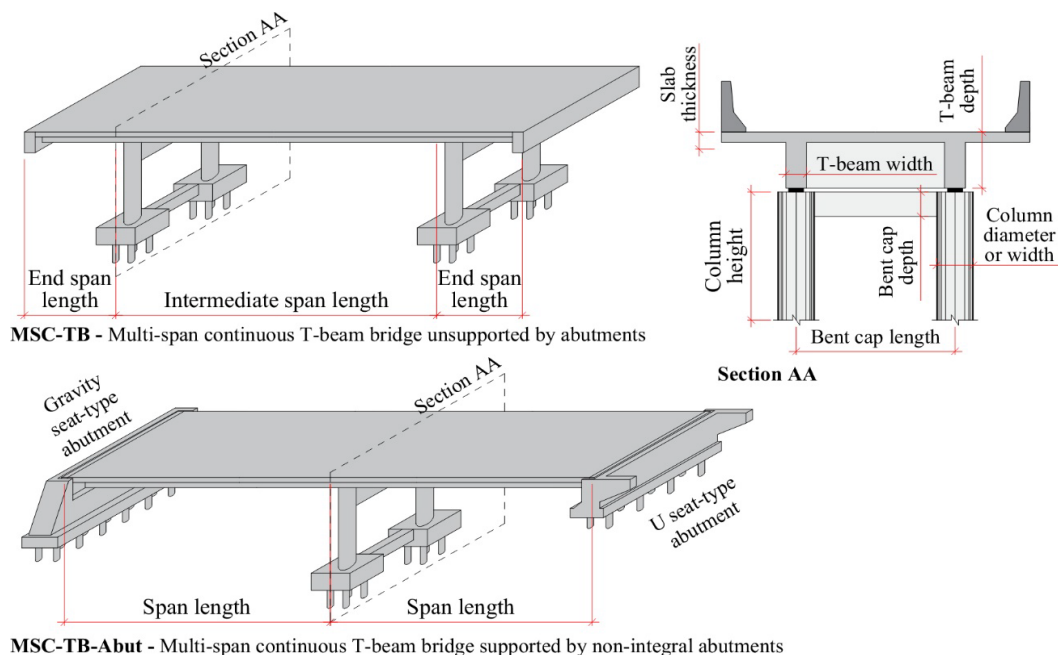


Figure 1. Geometric properties of the bridges' classes.

Several geometric features are adopted as variable to define each bridge’s class, such as: number of spans; span length; slab deck width and thickness; T-beam deck width; depth, width and slab thickness; column height and cross section dimensions; bent cap length, depth and width; abutment type and dimensions. Discrete and continuous distributions describe independent geometric variabilities (i.e., span length and column height). However, some parameter variabilities (i.e., T-beam depth and span length) are defined as a function of these independent variables, since strong correlations are observed in [35]. Pearson’s linear correlation coefficients (ρ_{xy}) are calculated and $\rho_{xy} > 0.7$ is assumed to indicate a strong correlation. The foundations, material properties and design details are not informed in the reports.

2.1.1 MSC-TB bridge’s class variability

Table 2 summarizes the characterization of the portfolio variabilities for the MSC-TB bridge’s classes. In addition, the widths of the T-beams and bent caps are assumed to be 0.4 m, as few reports present this information. Further details on distribution and function fits are available in [35]. Geometric parameters (e.g., intermediate span length) fitted by normal distributions are truncated using a 5% percentile cutoff point to avoid negative values, which are not physically representative.

Table 2. Characterization of the portfolio variabilities for the MSC-TB bridge’s class [35].

Variable	Distribution or function	Subclass	Parameters (m)
Number of spans (Ns)	Discrete	-	Ns = 3 (51.4%)
			Ns = 4 (11.4%)
			Ns = 5 (37.1%)
Intermediate span length (Lis)	Normal	-	$\mu = 18.24, \sigma = 4.79$ and $Lis \geq 10.4$
End span length (Les)	Linear regression	-	$Les(Lis) = 0.18 Lis + 1.03$
T-beam depth (Db)	Linear regression	-	$Db(Lis) = 0.05 Lis + 0.78$
Deck width (Dw)	Lognormal	-	$\lambda = 2.35$ and $\zeta = 0.14$
Bent cap length (Lbc)	Linear regression	-	$Lbc(Dw) = 0.56 Dw + 0.64$
Bent cap depth (Dbc)	Linear regression	-	$Dbc(Lbc) = 0.12 Lbc + 0.33$
Slab thickness (Sd)	Linear regression	-	$Sd(Lbc) = 0.04 Lbc$
Column height (Hc)	Lognormal	-	$\lambda = 1.25$ and $\zeta = 0.47$
Column diameter (Dc) or width (Wc)	Linear regression	1 ¹	$Dc(Lis) = 0.02 Lis + 0.37$
		2 ¹	$Wc(Lis) = 0.03 Lis + 0.25$

¹ Subclass 1 indicates bridges composed of circular columns with 73.7% occurrence

² Subclass 2 indicates bridges composed of rectangular columns with 26.3% occurrence

2.1.2 MSC-TB-Abut bridge’s class variability

The summary of the portfolio variabilities of the MSC-TB-Abut bridge’s class are illustrated in Table 3. According to the reports, some parameters are assumed to have constant values, such as the slab thickness of 0.3 m, deck width of 10 m, and the width and depth of the bent caps of 0.4 m and 1.0 m, respectively.

Table 3. Characterization of the portfolio variabilities for the MSC-TB-Abut bridge’s class [35].

Variable	Distribution or function	Subclass	Parameters (m)
Number of spans (Ns)	Discrete	-	Ns = 2 (66.7%)
			Ns = 3 (26.7%)
			Ns = 4 (6.6%)
Span length (Ls)	Lognormal	-	$\lambda = 2.7$ and $\zeta = 0.37$
T-beam depth (Db)	Linear regression	-	$Db(Ls) = 0.09 Ls + 0.07$
Bent cap length (Lbc)	Lognormal	-	$\lambda = 1.57$ and $\zeta = 0.04$
Column diameter (Dc)	Linear regression	-	$Dc(Ls) = 0.03 Ls + 0.36$
Column height (Hc)	Normal	-	$\mu = 4.82, \sigma = 1.58$ and $Hc \geq 1.66$
Abutment height (Ha)	Lognormal	1 ¹	$\lambda = 1.65$ and $\zeta = 0.41$
		2 ¹	$\lambda = 1.96$ and $\zeta = 0.13$

¹ Subclass 1 indicates gravity seat-type abutments with 42.9% occurrence

² Subclass 2 indicates U seat-type abutments with 57.1% occurrence

2.1.3 Material variability

Some parameters are not available in the DNIT database, such as compressive strength of concrete (f_c), steel yield stress (f_y) and steel Young's modulus (E_s). Their mean values (μ) and standard deviation (σ) are considered based on the literature, as shown in Table 4. Therefore, they are used as material variabilities to create different bridge samples. A conservative approach is used in the characterization of the f_c values, which is based on the C20 concrete class, since 77.7% of the age bridges recorded in DNIT reports were built up to 1975 [34]. Furthermore, the steel Young's Modulus is used as 210 GPa [36] for all analyses, as it has a small coefficient of variation value (i.e., about 3% in [37]).

Table 4. Material variability considered herein.

Variable	Distribution	Parameters	Reference
f_c (MPa)	Normal	$\mu = 26.2$ and $\sigma = 4.3$	Santiago and Beck [38]
f_y (MPa)	Normal	$\mu = 576$ and $\sigma = 46.1$	Nogueira [39]

Longitudinal and transverse reinforcement ratios for bent caps are calculated based on the minimum requirements of [36], since the T-beams are supported directly on the columns. A longitudinal reinforcement ratio of 1% is adopted for the columns according to [40] since Brazilian's bridges are usually not designed considering seismic detailing. Any other seismic details (e.g., shear keys, restrainer cables, elastomeric isolation bearing, steel jacket) were not seen in the reports, indicating that these seismic resistance features are not significantly used. In addition, transverse ties with diameters of 8 mm and a spacing of 20 cm ($\phi 8$ each 20) are used in the columns according to [36]. Note that column's reinforcement ratios are studied through parametric analyses in Subsection 4.4.

2.2 Numerical modeling

A generic finite-element (FE) model is created using OpenSees [41], which includes variation in geometric features and component modeling. The generic FE model is presented in Figure 2, where the dead loads from the superstructure are considered to be vertically concentrated at the top of the columns (force P).

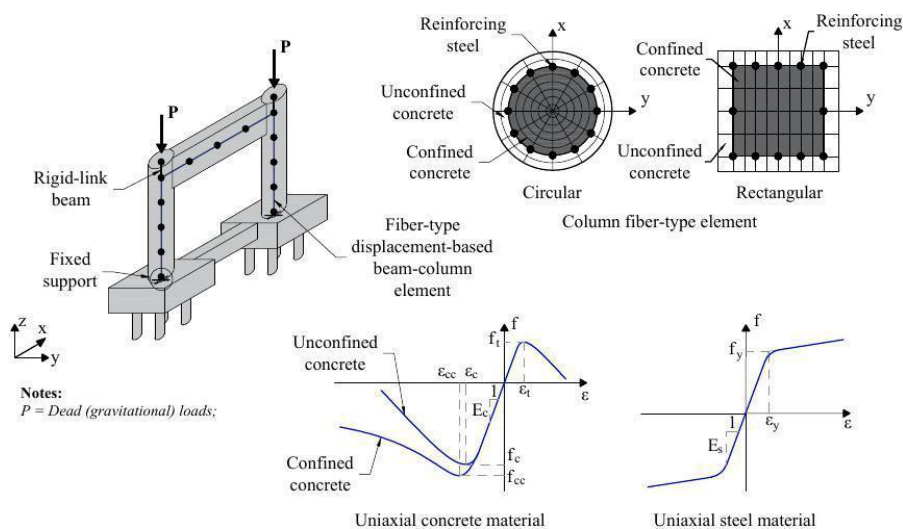


Figure 2. Generic FE model and nonlinear beam-column elements model behavior.

Rigid-link beams are used in vertical direction over the bridge piers to transfer lateral and gravitational loads from the deck to the bents. Bent beams and columns are modeled using fiber-type displacement-based beam-column elements with spread plasticity. The cross section of the element is divided into several fibers that delineate the regions of confined and unconfined concrete and the longitudinal reinforcement steel. The behavior of the uniaxial concrete material is based on the model proposed by [42], while the behavior of the reinforcement steel material is described by [43] with an isotropic strain-hardening ratio of 1%. Each column is divided into several elements along their height

with an approximate length of 50 centimeters and each bent beam and grade beam is divided into 4 elements along their length. The soil-structure interaction is not considered in the analysis and fixed support conditions are applied.

The numerical model is calibrated with the results of two cyclic experiments, as presented in Figure 3. The first is Experiment 5 by [44] in which a single column can simulate a lateral force acting in the longitudinal direction of the bridge. Meanwhile, the second experiment represents a frame composed of two columns [45] similar to the structural behavior of the bents in the transverse direction.

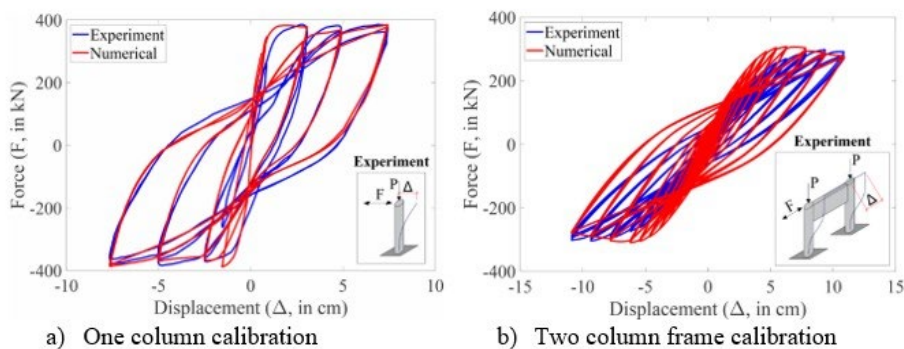


Figure 3. Numerical model calibration of the columns.

Note that hysteretic curves depicted in Figure 3 are in fair agreement. More information on the calibration can be found elsewhere [46], [47].

3 METHODOLOGY

In this section, the new methodology to estimate the structural capacity of the bridges' bents is described. It is proposed to replace the column's ductility ratio (μ) by a new parameter (e.g., curvature, drift) as an EDP. The methodology is divided into the following steps:

- Definition of the structural response to be adopted as the EDP, for example, section curvature (ϕ) or drift (θ). Note that this new EDP needs to be able to be written in function of the ductility ratio, as $EDP = \mu_{EDP} \times EDP_y$, where subscript y refers to the EDP values (e.g., ϕ or θ) in which the first longitudinal reinforcement yields. This approach allows the EDP to be obtained directly from the demand analysis, since it is not straightforward to obtain the column's yield parameter value in a portfolio analysis, because in some simulations yielding may not occur;
- Obtain from the literature, or develop, capacity models based on the column's ductility ratio that provide a clear relation between damage states. These capacity models are defined as median ($S_C[\mu_{EDP}|LS]$) and logarithmic dispersion ($\beta_C[\mu_{EDP}|LS]$) for each limit state (LS). These probabilistic distributions consider the uncertainties about the association between quantitative and qualitative damage states, as mentioned before. In addition, several authors adopt the capacity models based on lognormal distributions [11]-[16];
- Generate structural samples considering the variation of physical and geometric parameters to account for their variability within the bridges' classes;
- Perform PAs (or MPA if a bi-directional load scenario is required) in each structural sample to determine the EDP_y values;
- Fit the EDP_y values to a lognormal distribution, described by the median ($S_C[EDP_y]$) and the logarithmic dispersion ($\beta_C[EDP_y]$). One can also verify if the EDP_y values follow a lognormal distribution using a two-sample Kolmogorov-Smirnov (K-S) test. The dispersion obtained in these analyses would be based on the variability within the bridge's class, and this distribution is not yet associated to a LS;
- Assuming that there is no correlation between μ_{EDP} and EDP_y , the distribution of the structural capacity for each LS, given by a median S_C and a dispersion β_C , can be determined from the product between the distributions of μ_{EDP} and EDP_y , given by the following Equations 1 and 2 [48]:

$$S_C[EDP] = S_C[EDP_y] \times S_C[\mu_{EDP}|LS] \tag{1}$$

$$\beta_c[EDP] = \sqrt{\beta_c[EDP_y]^2 + \beta_c[\mu_{EDP}|LS]^2} \tag{2}$$

Figure 4 illustrates a summary of the proposed framework to determine the capacity model of bridge’s bents. As seen in Figure 4, the characterization of the EDP_y value is based on simultaneous monitoring of the EDP (i.e., section curvature, drift) values (pushover curve) and the steel stress (f) values of each longitudinal rebar (stress-strain curve) in the critical section at each PA step. In the step in which the first longitudinal rebar yields ($f=f_y$), the EDP value is equal to EDP_y .

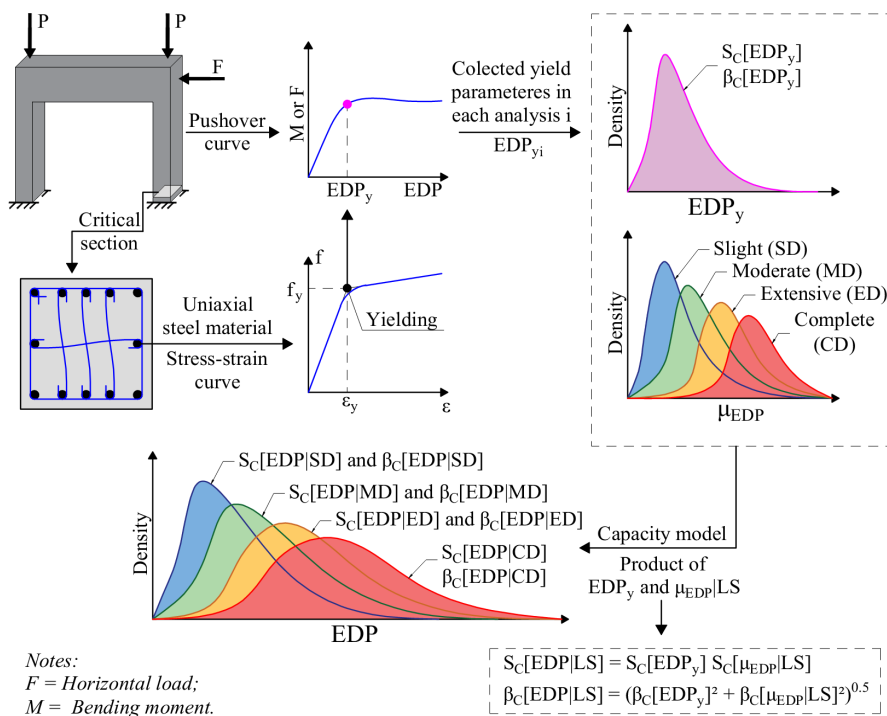


Figure 4. Methodology for defining a capacity model for bridge’s bents.

This framework allows a most adequate definition of the yield parameter through nonlinear analyses, and the consideration of the variability within a group of structures in the capacity model. In addition, Multidirectional Pushover Analyses (MPA) are performed to provide a better estimate of the yield parameter based on a bi-directional load scenario, as seen in Figure 5.

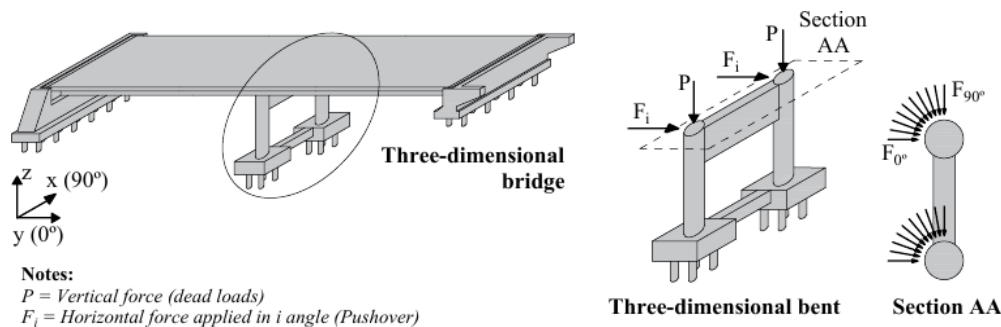


Figure 5. Direction of the horizontal force at the top of the bents.

The definition of qualitative damage states adopted herein follows [10] prescriptions (Table 5), which are divided into slight, moderate, extensive and complete damage.

Table 5. Description of damaged states.

Damage state	Description
Slight	Minor spalling at the column (damage requires no more than cosmetic repair)
Moderate	Any column experiencing moderate (shear cracks) cracking and spalling (column structurally still sound)
Extensive	Any column degrading without collapse – shear failure – (column structurally unsafe)
Complete	Any column collapsing

In order to obtain results from this methodology, 50 structural samples of bridges using the Latin-hypercube sampling (LHS) technique [49] are generated with variation of physical and geometric parameters to account for their variability within the bridges’ classes. The LHS is used to create a set of nominally identical but statistically different bridge samples, which considers a constrained sampling approach instead of randomly selected samples. The application of the LHS on the sampling of continuous distributions (independent parameters, e.g., span length, column height) is well known, and more information can be found elsewhere [50]. After sampling the independent parameters (e.g., span length), the dependent parameters described as linear functions (e.g., T-beam depth) are calculated. The sampling of the subclasses is performed based on the probability of occurrence, i.e., 73.7% (37 samples) of the columns of the MSC-TB class have a circular section and 26.3% (13 samples) have a rectangular section.

MPA are performed in each structural sample. In each analysis, the angle of application of the horizontal force is varied every 15° from 0° (bridge’s longitudinal direction) to 90° (transverse direction, i.e., bent’s plane). The yield curvature (ϕ_y) and the yield drift (θ_y) are selected as the yield parameters and are determined in each analysis.

The results of this research are presented in the next section, and divided into subsections, as described below:

- Comparison of the yield parameters (ϕ_y and θ_y) obtained in the MPA with the results of analytical equations proposed by [20]- [23]. This subsection intends to assess whether the use of analytical models properly estimates the yield parameters;
- Analysis of the influence of the bi-directional load scenario on the yield parameters (ϕ_y and θ_y). The main objective is to evaluate which parameter is less impacted by the variation of the angle of application of horizontal forces. These results help to select the most suitable yield parameter to generate the capacity models;
- Generation of limit state models for each bridge’s class based on the most suitable yield parameter using the proposed methodology in this article.;
- Parametric analysis considering different columns’ reinforcement ratio using MPA to determine the influence on the yield parameter (used in the above-mentioned analysis). The longitudinal reinforcement ratio is varied with values of 0.5%, 1.0%, 1.5% and 2%, and the transverse ties with diameters of 8, 10 and 12.5 mm and spacing of 20, 15 and 10 cm, respectively. From these results for each bridge’s class, analytical equations are proposed to extrapolate the yield parameter within a range of analyzed values for reinforcement ratios. Therefore, when this data (reinforcement ratios) is available, it will be possible to properly estimate the capacity of these columns.

4 RESULTS

4.1 Comparison of analytical and numerical models to obtain yield parameters

In this subsection, the adequacy of the adoption of analytical models to calculate yield parameters (ϕ_y and θ_y) is discussed. Priestley et al. [22] proposed Equations 3 and 4 to estimate ϕ_y and θ_y , respectively.

$$\phi_y = 2,25 \times \frac{\epsilon_y}{D_c} \tag{3}$$

$$\theta_y = \phi_y \times \frac{(H_c + L_{sp})^2}{3 \times H_c} \tag{4}$$

In Equation 3, ϵ_y is the yield strain of the longitudinal reinforcement and D_c is the column diameter. In Equation 4, H_c is the column height and L_{sp} is the strain penetration length, as defined in Equation 5.

$$L_{sp} = 0,022 \times f_y \times \Phi_{bl} \tag{5}$$

Where f_y is the longitudinal reinforcement yield strength and Φ_{bl} is the longitudinal reinforcement bar diameter. Note that these expressions are proposed for circular columns; therefore, the authors adapted them for rectangular columns by replacing D_c with W_c (column width).

The values of EDP_y (ϕ_y and θ_y) are calculated using the Equations 3 to 5 for each structural sample per bridge’s class, which are independent of the direction of analysis (e.g., longitudinal or transverse directions). Note that each sample provides unique parameter values (e.g., column height, column diameter, steel yield strength) to properly estimate one EDP_y . Each analytical result is related to each EDP_y obtained by the MPA for the seven angles of application of the horizontal force varying from 0° to 90° , as seen in Figure 6. In Figure 6, the vertical axes indicate the yield parameters obtained by the MPA divided by those calculated by the analytical models proposed by Priestley et al. [22], and the horizontal axes illustrate the results for each degree analyzed in the MPA.

The yield curvature results, shown in Figure 6, indicate that there is not a significant effect of the angle of application of forces on them, since the mean values range from 0.83 to 0.77 (about 8%) and from 0.86 to 0.84 (about 2%) for the MSC-TB and MSC-TB-Abut bridge’s classes, respectively. This influence on yield drift values is clearly stronger, as the same variations are around 857% (from 0.67 to 0.07) and 644% (from 0.67 to 0.09), respectively. The standard deviation of the MSC-TB results is higher due to the division of the class into circular and rectangular sections, and the greater number of variable geometric parameters (e.g., slab thickness, bent cap height), as detailed in Section 2.

All results in Figure 6 show that the yield parameters obtained with the analytical model are overestimated, except one sample that generated higher values of θ_y through the MPA (Figure 6d). This sample features a bridge with columns 1.7 m high and 1.4 m in diameter, which is unusual. Note that the LHS technique must be performed with uncorrelated parameters to adequately represent a large group of samples with small size data; therefore, it is common to provide a small number of samples with unusual characteristics.

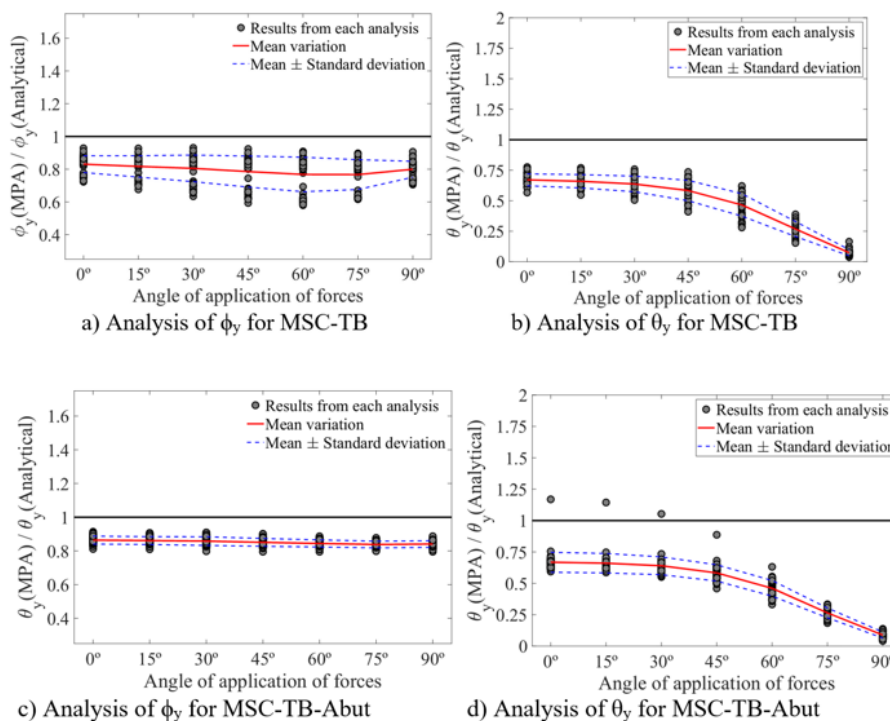


Figure 6. Relation between yield parameters obtained by MPA and by an analytical model proposed by Priestley et al. [22] for each angle of the MPA.

Other studies have also proposed analytical equations to estimate the yield curvature based on experimental results, such as Hernández-Montes and Aschleim [20] and Sheikh et al. [23]. [20] studied circular and rectangular columns and evaluated the influence of the axial load ratio on the yield curvature; while [23] evaluated circular columns to estimate equations based on the axial load ratio, longitudinal reinforcement ratio and compressive strength of concrete. Both models also consider the yield strain of the longitudinal reinforcement and the dimensions of the column’s cross section, as proposed by Priestley et al. [22]. In addition, Brachmann et al. [21] estimated the yield drift values as a function of the axial load ratio only.

A similar approach is also conducted to assess the suitability of using the analytical models [20]-[23] to estimate the yield parameters, which also utilizes the previous results from Figure 6. This intends to verify whether the EDP_y overestimation (i.e., using Priestley et al. [22] model) is also obtained using the aforementioned analytical models [20]-[21] and [23]. Therefore, longitudinal (0°) and transverse (90°) directions are evaluated based on the results obtained with the MPA. Figure 7 shows through box-and-whisker plots the comparison of yield parameters calculated from the equations proposed by [20]-[23] and determined with the MPA.

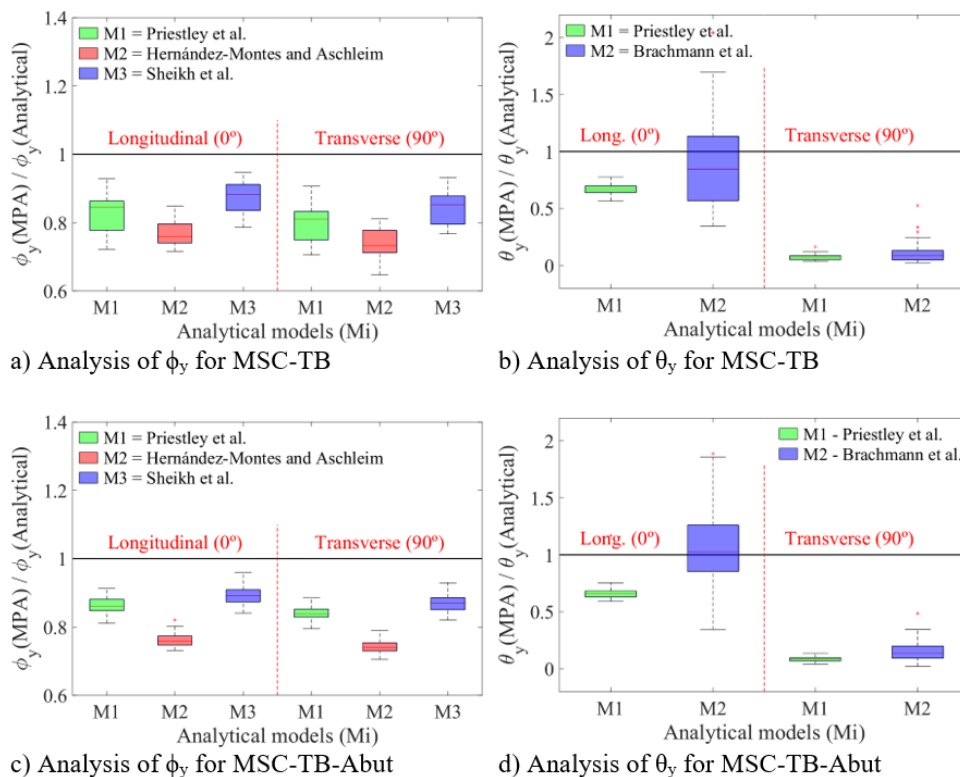


Figure 7. Relation between yield parameters obtained by MPA and by analytical models proposed by [20]-[23].

The results illustrated in Figure 7 indicate that the evaluated analytical equations overestimated the yield curvature. The model proposed by Sheik et al. [23] presented more accurate results, as more parameters are used to define ϕ_y . The results obtained using Hernández-Montes and Aschleim [20] are the least accurate, but with the smallest dispersion, which is consistent with the equations considering circular and rectangular columns. The yield drift results using Brachmann et al. [21] have a significantly greater dispersion, which is attributed to the single consideration of the axial load ratio in the equations; however, the results are more accurate with a lower tendency of overestimation.

Finally, the estimation of the yield parameters using analytical models may underestimate the fragility assessment of these bridge’s classes. Therefore, the employment of MPA is certainly a more accurate approach to estimating the capacity of bridge’s classes for a fragility assessment.

4.2 Comparison and selection of a most suitable EDP

This subsection presents an analysis of the appropriate EDP (i.e., ϕ_y or θ_y) to be adopted in the capacity models of the bridge’s bents considering a bi-directional load scenario. The MPA results of ϕ_y and θ_y for each degree of force application are described in Table 6, which includes the p-values of the two-sample K-S test. A significance level (α) of 0.05 is used [28], which means that the data follow a lognormal distribution if the $p\text{-value} \geq \alpha$.

Table 6. Comparison of ϕ_y and θ_y using the MPA for the bridge’s classes.

Yield parameter	Degree	MSC-TB			MSC-TB-Abut		
		S_c	β_c	p-value ¹	S_c	β_c	p-value ¹
ϕ_y (rad/m)	0°	0.0072	0.218	0.838	0.0068	0.228	0.498
	15°	0.0070	0.224	0.723	0.0068	0.228	0.573
	30°	0.0069	0.233	0.726	0.0068	0.231	0.597
	45°	0.0068	0.241	0.550	0.0067	0.228	0.632
	60°	0.0066	0.246	0.587	0.0066	0.226	0.625
	75°	0.0066	0.231	0.641	0.0066	0.223	0.716
	90°	0.0069	0.210	0.689	0.0066	0.220	0.615
θ_y (%)	0°	0.784	0.437	0.841	0.903	0.368	0.953
	15°	0.769	0.444	0.891	0.893	0.371	0.937
	30°	0.743	0.454	0.976	0.866	0.378	0.918
	45°	0.678	0.470	0.976	0.789	0.399	0.886
	60°	0.538	0.495	0.979	0.623	0.430	0.935
	75°	0.307	0.521	0.952	0.358	0.450	0.937
	90°	0.082	0.729	0.985	0.118	0.536	0.949

¹ These results indicate p-values from the two-sample K-S test.

The results indicate that the median values (S_c) of column yield curvatures are greater in longitudinal direction (0°) pushover analyses than in the transverse direction (90°). This is caused by the reduction of axial forces in the critical column when a transverse force or displacement is applied in the top of the bent, since the yielding of the longitudinal rebar occurs by excessive elongation. This reduction is directly related to the column height, since the bending moments generated by horizontal transverse forces (as a function of column height, bent cap length and number of columns) increase axial forces in an end column and decrease at the other extremity. The largest variations in median values and logarithmic dispersion are observed in the yield curvature of the MSC-TB bridge’s class, when the angle of the pushover analysis increases. Median values are up to 9.1% (from 0.0072 to 0.0066), and logarithmic dispersion up to 17.1% (from 0.246 to 0.210). For the MSC-TB-Abut bridge’s class, these variations are up to 3.0% and 5.0% for median values and logarithmic dispersions, respectively.

According to Table 6, the yield drift values are dependent on the angle of application of the forces, since variations of 856% in the median values (from 0.784% to 0.082%) and 66.8% in the dispersion values (from 0.437 to 0.729) are obtained for the longitudinal and transverse directions considering MSC-TB bridge’s class, respectively. This variation is related to the greater structural stiffness in the transverse direction. Finally, it is assumed that the data follow lognormal distributions, since all p-values are higher than the adopted significance level.

The conventional limit state models define lognormal distributions to describe a column's capacity, without distinguishing between longitudinal and transverse structural behavior [11]-[16]. Therefore, the results for these bridges’ classes indicate the curvature is a better EDP when the forces acting in both directions are significant, since the yield drift is more dependent on the angle’s direction. An alternative approach to use a drift-based EDP is to develop independent capacity models for longitudinal and transverse directions, as seen in other bridge components (e.g., bearings, abutments) [11]-[16]. Based on this discussion, the yield curvature is used in further analyses presented herein.

4.3 Column limit state capacities

This subsection presents new limit state capacity models for the bridge’s classes based on the assumption that there is no seismic detailing. The first step is to estimate the yield curvature parameter through lognormal distributions (i.e., S_c and β_c). Table 6 shows the probabilistic distributions for each degree of force application; however, only one distribution per bridge’s class must be used. Therefore, an attempt to gather all data (i.e., 7 degrees times 50 structural samples per bridge’s class) to be fitted by lognormal distributions is conducted. Figure 8 illustrates the results of fitting the data by lognormal distributions, graphically shown by empirical and lognormal cumulative distribution functions (CDF).

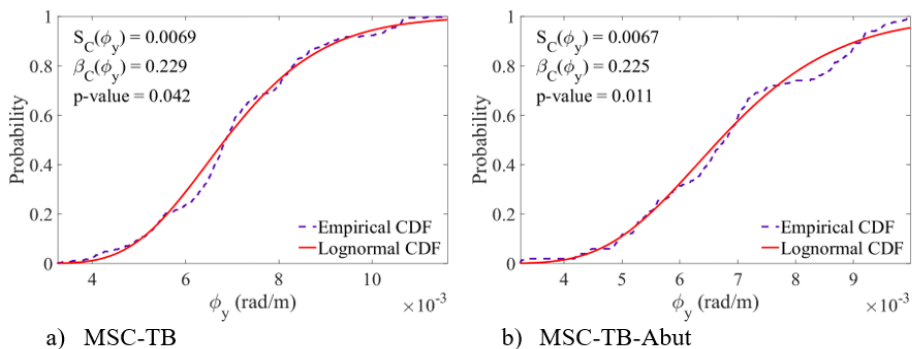


Figure 8. Two-sample K-S test results for the bridge’s classes, considering all data (350 analyses per class).

The results indicate that these data do not follow lognormal distributions ($p\text{-value} < \alpha$). Therefore, the mean values of ϕ_y are calculated for each structural sample, totaling 50 values of ϕ_y per bridge’s class, i.e., the mean results of the angle variations are used hereafter. The p-values results of the two-sample K-S test using mean values of ϕ_y are 0.857 and 0.537 for the MSC-TB and MSC-TB-Abut bridge’s classes, respectively. Table 7 presents the results of the parameters that describe the lognormal distributions of ϕ_y .

The next step on developing limit state capacity models is to define the probabilistic distributions of curvature ductility ratios. Therefore, the models proposed by [11] are used, since poorly confined concrete columns are adopted in the study. Using Equations 1 and 2, the column’s capacity models for each bridge’s class are proposed, as seen in Table 7.

Table 7. Column’s capacity models for typical bridges in Northeastern Brazil.

Bridge’s class	Damage state	$\mu_{\phi LS}$		ϕ_y		EDP: ϕ_{LS}^1	
		$S_C[\mu_{\phi}]$	$\beta_C[\mu_{\phi}]$	$S_C[\phi_y]$	$\beta_C[\phi_y]$	$S_C[\phi]$	$\beta_C[\phi]$
MSC-TB	Slight	1.29	0.59	0.0069	0.227	0.0089	0.632
	Moderate	2.10	0.51			0.0145	0.558
	Extensive	3.52	0.64			0.0243	0.679
	Complete	5.24	0.65			0.0362	0.688
MSC-TB-Abut	Slight	1.29	0.59	0.0067	0.226	0.0086	0.632
	Moderate	2.10	0.51			0.0141	0.558
	Extensive	3.52	0.64			0.0236	0.679
	Complete	5.24	0.65			0.0351	0.688

¹ Indicates the proposed column’s capacity model

Figure 9 illustrates the probability density functions (PDF) for column’s limit state models of each bridge’s class. These capacity models may be used for further fragility assessments of this bridge inventory.

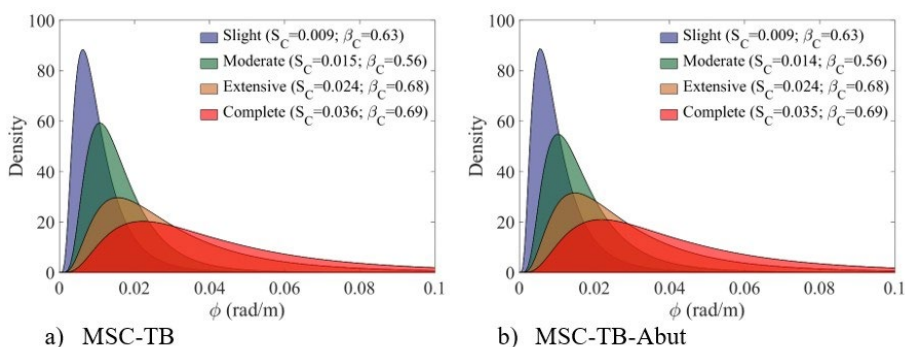


Figure 9. PDF for column’s capacity models.

4.4 Parametric analyses

This subsection presents a parametric analysis of column reinforcement ratios (i.e., longitudinal and transverse) to study their impact on the yield curvature (ϕ_y). Note that these ratios are unknown on a regional scale, and these results intend to extrapolate limit state capacities of columns. All results presented herein consider the variation of the angle of application of the forces (i.e., mean values of ϕ_y) and its influence is not evaluated separately.

An approach similar to the one presented in Section 4.3 is used, where the same 50 structural samples per bridge’s class are analyzed varying the angle of application by 15° to perform the PA with each reinforcement configuration. Table 8 presents the results of the yielding curvature for each configuration of longitudinal reinforcement ratio and transverse ties.

Table 8. Yielding curvature results for different reinforcement ratios.

Longitudinal reinforcement ratio (ρ)	Distribution of transverse ties	Yielding curvature (rad/m)			
		MSC-TB		MSC-TB-Abut	
		S_c	β_c	S_c	β_c
0,50%	$\phi 8$ s/20	0.00659		0.00642	
	$\phi 10$ s/15	0.00664	0.223	0.00646	0.223
	$\phi 12.5$ s/10	0.00668		0.00649	
1,00%	$\phi 8$ s/20	0.00683		0.00665	
	$\phi 10$ s/15	0.00687	0.225	0.00669	0.226
	$\phi 12.5$ s/10	0.00691		0.00672	
1,50%	$\phi 8$ s/20	0.00706		0.00686	
	$\phi 10$ s/15	0.00711	0.228	0.00691	0.229
	$\phi 12.5$ s/10	0.00714		0.00693	
2,00%	$\phi 8$ s/20	0.00726		0.00706	
	$\phi 10$ s/15	0.00730	0.230	0.0071	0.229
	$\phi 12.5$ s/10	0.00733		0.00713	

The variation in dispersion due to the increase of the transverse reinforcement ratio is less than 0.4%, which is neglected in the results. The average variation in the median of the yield curvature due to the increase of the lower to the upper values of the transverse reinforcement ratio is 1.09%, which is about ten times less than the average variation due to the increase in the longitudinal reinforcement ratio (9.93%). By increasing the longitudinal reinforcement four times, the dispersion varies up to 3.14%. Therefore, the increase in the transverse reinforcement ratio does not significantly influence the yield curvature results, which agrees with the results observed in [51]; however, the confinement effect may increase the ductility demand ratios (or capacity ratios) associated with each limit state (Table 7), which is not considered herein. Experimental results indicate that increasing the transverse reinforcement ratio causes an increase in ductility levels, dissipated energy and equivalent viscous damping [51], since the role of stirrups is to enhance confinement effect, to restrain the lateral expansion of concrete, thus modifying the concrete stress-strain constitutive law and enabling higher compression strains and higher ductility [52].

Using all the analysis results, a linear regression is performed in the logarithmic space to determine median values of the yield curvature (S_c) as a function of the longitudinal reinforcement ratio (ρ), as presented in Figure 10, since the impact of the transverse reinforcement ratio is neglected. Furthermore, the logarithmic standard deviation is assumed to have a constant value (Equation 7), which is consistent with the low variation obtained, as shown in Table 7. The linear relation is established (Equation 6), where a and b are the regression coefficients.

$$\ln(S_c) = \ln(a) + b \times \ln(\rho) \tag{6}$$

The logarithmic standard deviation of the capacity (β_c) is calculated through the same linear regression, as shown in Equation 4.

$$\beta_c \cong \sqrt{\frac{\sum[\ln(\phi_{yi}) - \ln(a \times \rho^b)]^2}{N-2}} \tag{7}$$

where N is the number of simulations and ϕ_{yi} are the mean yield curvature values of each simulation i . The dispersion values determined are constant (0.23) and compatible with those found in Table 7.

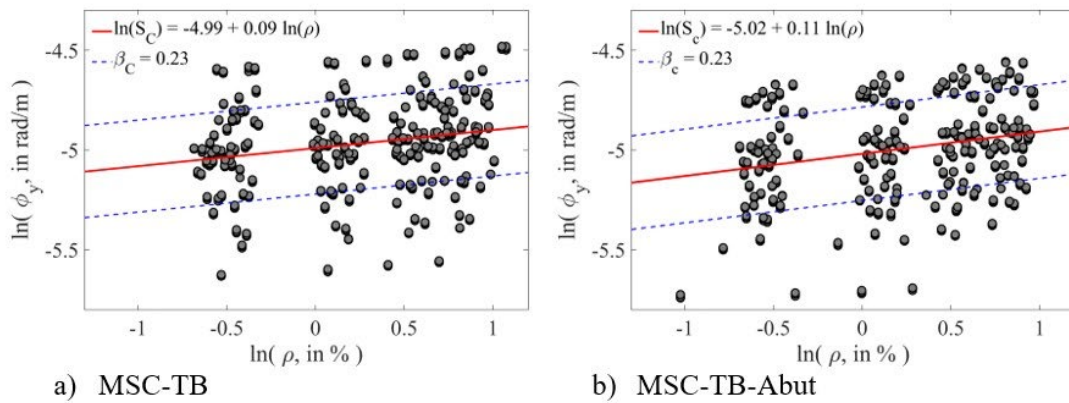


Figure 10. Linear regression of the median values of ϕ_y as a function of ρ .

Equations 8 and 9 define the relationship between the median values of ϕ_y and ρ for the MSC-TB and MSC-TB-Abut bridges' classes, respectively. Therefore, it allows defining the distribution of capacity for different values of the longitudinal reinforcement ratios.

$$\ln(S_c) = -4.99 + 0.09 \times \ln(\rho) \tag{8}$$

$$\ln(S_c) = -5.02 + 0.11 \times \ln(\rho) \tag{9}$$

5 CONCLUSIONS

This article presents a new proposal to estimate the structural capacity analysis for typical bridge bents in Northeastern Brazil. Multidirectional pushover analyses are performed to assess the influence of the angle of application of the force in the bridge bents. Drift and curvature are evaluated as yield parameters for excitation loads that occur at two horizontal component forces (i.e., earthquakes). The results of analytical models used herein overestimate the yield parameters when compared to the MPA results. In addition, the yield drift is more sensitive to the angle of application of the forces, which presents a variation up to 856% in the median drift values obtained in the longitudinal and transverse directions to the first reinforcement yielding of the critical section. Therefore, the curvature is adopted as EDP for the new methodology proposed here, as it presents a better performance in a multidirectional pushover analysis with less variation in the results (up to 19%). Finally, capacity limit states are provided, considering uncertainties about the association between quantitative and qualitative damage states and variability within the bridge's classes.

Parametric analyses are performed to assess the impact of longitudinal and transverse reinforcement ratios on the structural capacity of the bents. The results show that the variation in the longitudinal reinforcement ratio has a greater influence on the yield curvature. The definition of the ductility demand ratios for the bridge portfolio is a gap in the study, since values suggested in the literature are adopted for other bridge configurations. The results of the parametric analyses enable the generation of linear relations between the yield curvature and the reinforcement ratios. Such relations are useful to estimate capacity models for probabilistic or deterministic vulnerability assessments ([11]-[17] and [53]) or displacement-based design procedures [54]. The former is particularly useful in Brazil, given the lack of studies that developed such relations, and the variety of old and new bridges designed according to different codes (consequently, different reinforcement ratios).

The capacity limit states obtained herein are valuable information to perform a vulnerability analysis of the bridge portfolio by several different hazard sources, such as earthquakes, hurricanes and explosions. In addition, these results may be used in other bridge portfolios with geometric and physical characteristics similar to the bridge bents analyzed herein.

ACKNOWLEDGEMENTS

This study was financed in part by the Coordenação de Aperfeiçoamento de Pessoal de Nível Superior - Brasil (CAPES) - Finance Code 001; and by the São Paulo Research Foundation (FAPESP) - Finance Code 2018/23304-9. The opinions, findings, and conclusions or recommendations expressed in this paper are those of the authors only and do not necessarily reflect the views of the sponsors or affiliates.

REFERENCES

- [1] F. Schanack, G. Valdebenito, and J. Alvial, "Seismic damage to bridges during the 27 February 2010 magnitude 8.8 Chile earthquake," *Earthq. Spectra*, vol. 28, no. 1, pp. 301–315, 2012, <http://dx.doi.org/10.1193/1.3672424>.
- [2] A. Palermo et al., "Performance of road bridges during the 14 November 2016 Kaikoura earthquake," *Bull. N. Zeland Soc. Earthq. Eng.*, vol. 50, no. 2, pp. 253–270, 2017, <http://dx.doi.org/10.5459/bnzsee.50.2.253-270>.
- [3] Y. Alberto, M. Otsubo, H. Kyokawa, T. Kiyota, and I. Towhata, "Reconnaissance of the 2017 Puebla, Mexico earthquake," *Soil Found.*, vol. 58, no. 5, pp. 1073–1092, 2018, <http://dx.doi.org/10.1016/j.sandf.2018.06.007>.
- [4] N. Ataei and J. E. Padgett, "Probabilistic modeling of bridge deck unseating during hurricanes events," *J. Bridge Eng.*, vol. 18, no. 4, pp. 275–286, 2013, [http://dx.doi.org/10.1061/\(ASCE\)BE.1943-5592.0000371](http://dx.doi.org/10.1061/(ASCE)BE.1943-5592.0000371).
- [5] N. Ataei and J. E. Padgett, "Fragility surrogate models for coastal bridges in hurricane prone zones," *Eng. Struct.*, vol. 103, pp. 203–213, 2015, <http://dx.doi.org/10.1016/j.engstruct.2015.07.002>.
- [6] G. P. Balomenos, S. Kameshwar, and J. E. Padgett, "Parameterized fragility models for multi-bridges' classes subjected to hurricane loads," *Eng. Struct.*, vol. 208, pp. 110213, 2020, <http://dx.doi.org/10.1016/j.engstruct.2020.110213>.
- [7] F. H. B. Alves "Sistema de previsão de enchentes: integração de modelos de previsão de chuva, simulação hidrológica e hidrodinâmica," M.S. thesis, Universidade Federal de Pernambuco, UFPE, Pernambuco, Brasil, 2017.
- [8] F. H. B. Alves "Análise dos níveis de solicitação gerados por explosivos sobre os pilares do viaduto da BR-020 em Caucaia, Ceará, aliada à verificação de segurança e dimensionamento preventivo," B.S. thesis, Universidade Federal do Ceará, UFCE, Ceará, Brasil, 2019.
- [9] J. E. Padgett and R. DesRoches, "Methodology for the development of analytical fragility curves for retrofitted bridges," *Earthquake Eng. Struct. Dynam.*, vol. 37, no. 8, pp. 1157–1174, 2008, <http://dx.doi.org/10.1002/eqe.801>.
- [10] Federal Emergency Management Agency, *Earthquake Loss Estimation Methodology, HAZUS-MH 2.1: Technical Manual*. Washington, DC, USA: FEMA, 1997.
- [11] B. G. Nielson and R. DesRoches, "Seismic fragility methodology for highway bridges using a component level approach," *Earthquake Eng. Struct. Dynam.*, vol. 36, no. 6, pp. 823–839, 2007, <http://dx.doi.org/10.1002/eqe.655>.
- [12] H. Pahlavan, B. Zakeri, G. G. Amiri, and M. Shaijanfar, "Probabilistic vulnerability assessment of horizontally curved multiframe RC box-girder highway bridges," *J. Perform. Constr. Facil.*, vol. 30, no. 3, pp. 04015038, 2016, [http://dx.doi.org/10.1061/\(ASCE\)CF.1943-5509.0000780](http://dx.doi.org/10.1061/(ASCE)CF.1943-5509.0000780).
- [13] E. Choi, R. DesRoches, and B. Nielson, "Seismic fragility of typical bridges in moderate seismic zones," *Eng. Struct.*, vol. 26, pp. 187–199, 2004, <http://dx.doi.org/10.1016/j.engstruct.2003.09.006>.
- [14] K. Ramanathan, R. DesRoches, and J. E. Padgett, "Analytical fragility curves for multispan continuous steel girder bridges in moderate seismic zones," *Transp. Res. Rec.*, vol. 2202, no. 1, pp. 173–182, 2010, <http://dx.doi.org/10.3141/2202-21>.
- [15] H. Pahlavan, B. Zakeri, G. G. Amiri, and M. Shaijanfar, "Probabilistic vulnerability assessment of horizontally curved multiframe RC box-girder highway bridges," *J. Perform. Constr. Facil.*, vol. 30, no. 3, pp. 04015038, 2016, <http://dx.doi.org/10.1061/%28ASCE%29CF.1943-5509.0000780>.
- [16] S. Mangalathu, F. Soleimani, and J.-S. Jeon, "Bridge's classes for regional seismic risk assessment: Improving hazus models," *Eng. Struct.*, vol. 148, pp. 755–766, 2017, <http://dx.doi.org/10.1016/j.engstruct.2017.07.019>.
- [17] J. E. Padgett and R. DesRoches, "Bridge functionality relationships for improved seismic risk assessment of transportation networks," *Earthq. Spectra*, vol. 23, no. 1, pp. 115–130, 2007, <http://dx.doi.org/10.1193/1.2431209>.
- [18] A. Dutta and J. B. Mander, "Seismic fragility analysis of highway bridges," in *Proceedings of the Center-to-Center Project Workshop on Earthquake Engineering in Transportation System*, Tokyo, Japan, 1999.
- [19] H. Hwang, J. B. Liu, and Y.-H. Chiu, *Seismic Fragility Analysis of Highway Bridges* (Mid-America Earthquake Center Tech. Rep. MAEC RR-4 Project), USA: University of Memphis, 2001.
- [20] E. Hernández-Montes and M. Aschleim, "Estimates of the yield curvature for design of reinforced concrete columns," *Mag. Concr. Res.*, vol. 55, no. 4, pp. 337–383, 2003, <http://dx.doi.org/10.1680/macr.2003.55.4.373>.
- [21] I. Brachmann, J. Browning, and A. Matamoros, "Drift-dependent confinement requirements for reinforced concrete columns under cyclic loading," *ACI Struct. J.*, vol. 101, no. 5, pp. 669–677, 2004, <http://dx.doi.org/10.14359/13389>.

- [22] M. N. Priestley, G. M. Calvi, and M. J. Kowalsky, *Displacement Based Seismic Design of Structures*, 1st ed. Pavia: IUSS Press, 2007.
- [23] M. N. Sheik, H. S. Tsang, T. J. McCarthy, and N. T. K. Lam, "Yield curvature for seismic design of circular reinforced concrete columns," *Mag. Concr. Res.*, vol. 62, no. 10, pp. 741–748, 2010, <http://dx.doi.org/10.1680/mac.2010.62.10.741>.
- [24] D. H. Tavares, J. R. Suescun, P. Paultre, and J. E. Padgett, "Seismic fragility of a highway bridge in Quebec," *J. Bridge Eng.*, vol. 18, no. 11, pp. 1131–1139, 2013, [http://dx.doi.org/10.1061/\(asce\)be.1943-5592.0000471](http://dx.doi.org/10.1061/(asce)be.1943-5592.0000471).
- [25] B. R. Aryal and N. C. Sharma, "Development of fragility curves for seismic performance comparison of hammerhead and multicolumn bridge pier," *Int. J. Sci. Res.*, vol. 9, no. 3, pp. 3–8, 2020, <http://dx.doi.org/10.21275/SR20209224222>.
- [26] H. Krawinkler and G. D. P. K. Seneviratna, "Pros and cons of a pushover analysis of seismic performance evaluation," *Eng. Struct.*, vol. 20, no. 4–6, pp. 452–464, 1998, [http://dx.doi.org/10.1016/s0141-0296\(97\)00092-8](http://dx.doi.org/10.1016/s0141-0296(97)00092-8).
- [27] T. Isakovic and M. Fischinger, "Higher modes in simplified inelastic seismic analysis of single column bent viaducts," *Earthquake Eng. Struct. Dynam.*, vol. 35, no. 1, pp. 95–114, 2006, <http://dx.doi.org/10.1002/eqe.535>.
- [28] M. S. C. Garcia, G. H. Siqueira, L. C. M. Vieira Jr., and I. Vizotto, "Evaluation of structural capacity of triangular and hexagonal reinforced concrete free-form shells," *Eng. Struct.*, vol. 188, pp. 519–537, 2019, <http://dx.doi.org/10.1016/j.engstruct.2019.03.044>.
- [29] H. Rodrigues, H. Varum, A. Arêde, and A. Costa, "Comparative efficiency analysis of different nonlinear modelling strategies to simulate the biaxial response of RC columns," *Earthq. Eng. Eng. Vib.*, vol. 11, no. 4, pp. 553–566, 2012, <http://dx.doi.org/10.1007/s11803-012-0141-1>.
- [30] H. Rodrigues, A. Arêde, H. Varum, and A. Costa, "Experimental evaluation of rectangular reinforced concrete column behaviour under biaxial cyclic loading," *Earthquake Eng. Struct. Dynam.*, vol. 42, no. 2, pp. 239–259, 2012, <http://dx.doi.org/10.1002/eqe.2205>.
- [31] D. Giardini, P. Basham, and M. Bery, "The global seismic hazard assessment program (GSHAP) – 1992/1999," *Ist. Naz. Geofis. Vulcanologia*, vol. 42, no. 6, pp. 957–974, 1999, <http://dx.doi.org/10.4401/ag-3780>.
- [32] M. Assumpção, M. Pirchiner, J. Dourado, and L. Barros, "Terremotos no Brasil: preparando-se para eventos raros," *Boletim SBGf*, no. 96, pp. 25–29, 2016.
- [33] M. D. Petersen et al., "Seismic hazard, risk, and design for South America," *Bull. Seismol. Soc. Am.*, vol. 108, no. 2, pp. 781–800, 2018, <http://dx.doi.org/10.1785/0120170002>.
- [34] C. B. L. Oliveira, M. Greco, and T. N. Bittencourt, "Analysis of the Brazilian federal bridge inventory," *IBRACON Struct. Mater. J.*, vol. 12, no. 1, pp. 1–13, 2019, <http://dx.doi.org/10.1590/s1983-41952019000100002>.
- [35] G. H. F. Cavalcante, E. M. V. Pereira, I. D. Rodrigues, L. C. M. Vieira Jr., J. E. Padgett, and G. H. Siqueira "Proposal of representative portfolios for federal roadway bridges in Northeastern Brazil," Preprint arXiv:2108.00934, 2021.
- [36] Associação Brasileira de Normas Técnicas, *Projeto de Estruturas de Concreto - Procedimento*, NBR 6118, 2014.
- [37] S. A. Mirza and J. G. MacGregor, "Variability of mechanical properties of reinforcing bars," *J. Struct. Div.*, vol. 105, no. 5, pp. 921–937, 1979.
- [38] W. Santiago and A. Beck, "A new study of Brazilian concrete strength conformance," *IBRACON Struct. Mater. J.*, vol. 10, no. 4, pp. 906–923, 2017, <http://dx.doi.org/10.1590/s1983-41952017000400008>.
- [39] C. G. Nogueira "Desenvolvimento de modelos mecânicos de confiabilidade e de otimização para aplicação em estruturas de concreto armado," Ph.D. thesis, Departamento de Engenharia, Universidade de São Paulo, USP, São Paulo, Brasil, 2010.
- [40] J. E. Padgett and R. DesRoches, "Retrofitted bridge fragility analysis for typical classes of multispan bridges," *Earthq. Spectra*, vol. 25, no. 1, pp. 117–141, 2009, <http://dx.doi.org/10.1193/1.3049405>.
- [41] S. Mazzoni et al., "Open system for earthquake engineering simulation: OpenSees Command Language Manual." <https://opensees.berkeley.edu/OpenSees/manuals/usermanual/OpenSeesCommandLanguageManual.pdf> (accessed Jan. 26, 2021).
- [42] G. A. Chang and J. B. Mander, *Seismic Energy Based Fatigue Damage Analysis of Bridge Columns: Part 1 – Evaluation of Seismic Capacity* (Tech. Rep. NCEER-94-006). Buffalo NY, USA: National Center for Earthquake Engineering Research, 1994.
- [43] F. C. Filippou, V. V. Bertero, and E. P. Popov, *Effects of Bond Deterioration on Hysteretic Behavior of Reinforced Concrete Joints* (Tech. Rep. NSF/CEE-83032). Berkeley, CA, USA: Earthquake Engineering Research Center, 1983.
- [44] H. Tanaka, "Effect of lateral confining reinforcement on the ductile behavior of reinforced concrete columns," Ph.D. thesis, University of Canterbury, New Zealand, 1990.
- [45] P. Morandi, S. Hak, and G. Magenes, "Performance-based interpretation of in-plane cyclic tests on RC frames with strong masonry infills," *Eng. Struct.*, vol. 156, pp. 503–521, 2018, <http://dx.doi.org/10.1016/j.engstruct.2017.11.058>.
- [46] E. M. V. Pereira, "Estudo da fragilidade sísmica de pórticos de concreto armado com irregularidades estruturais," M.S. thesis, Unicamp, Campinas, SP, 2021. [Online]. Available: <http://repositorio.unicamp.br/Busca/Download?codigoArquivo=464788>
- [47] E. M. V. Pereira, G. H. F. Cavalcante, I. D. Rodrigues, L. C. M. Vieira Jr., and G. H. Siqueira, "Seismic reliability assessment of a non-seismic reinforced concrete framed structure designed according to ABNT NBR 6118:2014," *IBRACON Struct. Mater. J.*, vol. 15, no. 1, pp. e15110, 2022, <http://dx.doi.org/10.1590/S1983-41952022000100010>.
- [48] A. T. Beck, *Confiabilidade e Segurança das Estruturas*, 1th ed. Elsevier, Brasil, 2019.

- [49] M. D. McKay, R. J. Beckham, and W. J. Conover, "Comparison of three methods for selecting values of input variables in the analysis of output from a computer code," *Technometrics*, vol. 21, no. 2, pp. 239–245, 1979, <http://dx.doi.org/10.2307/1271432>.
- [50] O. Avsar, "Fragility based seismic vulnerability assessment of ordinary highway bridges in Turkey," Ph.D. thesis, Middle East Technical University, Ankara, Turkey, 2009.
- [51] M. A. Belkacem, H. Bechtoula, N. Bourahla, and A. A. Belkacem, "Effect of axial load and transverse reinforcements on the seismic performance of reinforced concrete columns," *Front. Struct. Civ. Eng.*, vol. 13, no. 4, pp. 831–851, 2019, <http://dx.doi.org/10.1007/s11709-018-0513-3>.
- [52] D. Domenico, D. Falliano, and G. Ricciardi, "Confinement effect of different arrangements of transverse reinforcement on axially loaded concrete columns: An experimental study," *J. Mech. Behav. Mater.*, vol. 28, no. 1, pp. 13–19, 2019, <http://dx.doi.org/10.1515/jmbm-2019-0003>.
- [53] A. Deb, A. L. Zha, Z. A. Caamaño-Withall, J. P. Conte, and J. I. Restrepo, "Updated probabilistic seismic performance assessment framework of ordinary standard bridges in California," *Earthquake Eng. Struct. Dynam.*, vol. 50, no. 9, pp. 2551–2570, 2021, <http://dx.doi.org/10.1002/eqe.3459>.
- [54] R. W. Soares, S. S. Lima, and S. H. C. Santos, "Reinforcement concrete bridge pier ductility analysis for different levels of detailing," *IBRACON Struct. Mater. J.*, vol. 10, no. 5, pp. 1042–1050, 2017, <http://dx.doi.org/10.1590/s1983-41952017000500006>.

Author contributions: GHFC: conceptualization, data curation, methodology, formal analysis, software, writing-original draft; EMVP: methodology, formal analysis, writing-original draft; IDR: methodology, formal analysis, writing-original draft; LCMVJ: Project administration; GHS: Project administration, formal analysis, supervision, writing-review & editing.

Editors: Mauricio Ferreira, Guilherme Aris Parsekian.